nature chemical biology

Cytochrome *c* acts as a cardiolipin oxygenase required for release of proapoptotic factors

Valerian E Kagan[1], Vladimir A Tyurin[1], Jianfei Jiang[1], Yulia Y Tyurina[1], Vladimir B Ritov[1], Andrew A Amoscato[2], Anatoly N Osipov[1], Natalia A Belikova[1], Alexandr A Kapralov[1], Vidisha Kini[1], Irina I Vlasova[1], Qing Zhao[1], Meimei Zou[1], Peter Di[1], Dimitry A Svistunenko[3], Igor V Kurnikov[1] & Gregory G Borisenko[1,4]

Programmed death (apoptosis) is turned on in damaged or unwanted cells to secure their clean and safe self-elimination. The initial apoptotic events are coordinated in mitochondria, whereby several proapoptotic factors, including cytochrome *c*, are released into the cytosol to trigger caspase cascades. The release mechanisms include interactions of B-cell/lymphoma 2 family proteins with a mitochondria-specific phospholipid, cardiolipin, to cause permeabilization of the outer mitochondrial membrane. Using oxidative lipidomics, we showed that cardiolipin is the only phospholipid in mitochondria that undergoes early oxidation during apoptosis. The oxidation is catalyzed by a cardiolipin-specific peroxidase activity of cardiolipin-bound cytochrome *c*. In a previously undescribed step in apoptosis, we showed that oxidized cardiolipin is required for the release of proapoptotic factors. These results provide insight into the role of reactive oxygen species in triggering the cell-death pathway and describe an early role for cytochrome *c* before caspase activation.

Irreparably damaged, genetically modified or unwanted cells are eliminated through a carefully regulated biochemical death program, or apoptosis. General principles of the apoptotic program, particularly its execution segment, have been deciphered, but the specific details of triggering events remain less clear. In vertebrate cells, the most common form of apoptosis proceeds through the mitochondrial (intrinsic) death pathway[1]. This pathway is activated by a diversity of chemicals, drugs, and X- and UV-irradiation capable of inducing cell stress, particularly DNA damage. After activation of this pathway, the release of several proapoptotic proteins—including cytochrome *c* (cyt *c*) and Smac/Diablo—from the intermembrane space of mitochondria into the cytosol, associated with mitochondrial membrane permeabilization, is the key event leading to the activation of caspases[2]. Released cyt *c* directly binds to and activates Apaf-1, which then facilitates the activation of the initiator, caspase—9, followed by the activation of the effector, caspase-3. Smac/Diablo removes the inhibition of caspase-3 and caspase-9 by inhibitor of apoptosis proteins (IAPs). A mitochondria-specific phospholipid, cardiolipin (CL), probably interacting with the members of the B-cell/lymphoma 2 (Bcl-2) family, is involved in permeabilization of the outer mitochondrial membrane and cyt *c* release[1,3,4], and a growing body of evidence implicates CL peroxidation products over nonoxidized CL as the real players in mitochondrial cyt *c* release[5–7]. Yet mechanisms of apoptosis-driven CL oxidation remain unknown. We showed that a pool of CL-bound mitochondrial cyt *c* functions as a peroxidase, catalyzing CL peroxidation that is required for release of cyt *c* and other proapoptotic factors from mitochondria.

RESULTS

Early and selective CL oxidation during apoptosis

We used an oxidative lipidomics approach to assess oxidation of different classes of phospholipids in cells during intrinsic apoptosis. Two relatively minor phospholipids—CL and phosphatidylserine (PS)—which both share an anionic character, underwent oxidation after stimulation of human myelogenous leukemia HL-60 cells or mouse embryonic cells by proapoptotic stimuli, staurosporine (STS) and actinomycin D (ACD), respectively. Two more abundant phospholipids, phosphatidylethanolamine (PE) and phosphatidylcholine (PC), did not undergo any oxidation under the same conditions (**Fig. 1a**). In mammalian cells, molecular species of PE and PC with arachidonic ($C_{20:4}$), eicosapentaenoic ($C_{20:5}$) and docosahexaenoic ($C_{22:6}$) acyls—which are particularly susceptible to peroxidation[8]—constitute 30–40 mol% and ~10 mol%, respectively[9–12], whereas CL contains predominantly less oxidizable linoleic acid ($C_{18:2}$) residues. Yet, CL rather than PE or PC was oxidized in cells during apoptosis, suggesting that CL oxidation was nonrandom and catalyzed by an apoptosis-specific mechanism. Given that PS is essentially absent from mitochondria (<1 mol%), CL was the only mitochondrial phospholipid that underwent peroxidation during apoptosis.

[1]Center for Free Radical and Antioxidant Health and Department of Environmental and Occupational Health, and [2]Department of Pathology, University of Pittsburgh, Pittsburgh, Pennsylvania 15260, USA. [3]Department of Biological Sciences, University of Essex, Wivenhoe Park, Colchester, Essex CO4 3SQ, UK. [4]Research Institute of Physico-Chemical Medicine, Moscow 119992, Russia. Correspondence should be addressed to V.E.K. (vkagan@eoh.pitt.edu).

Published online 14 August 2005; doi:10.1038/nchembio727

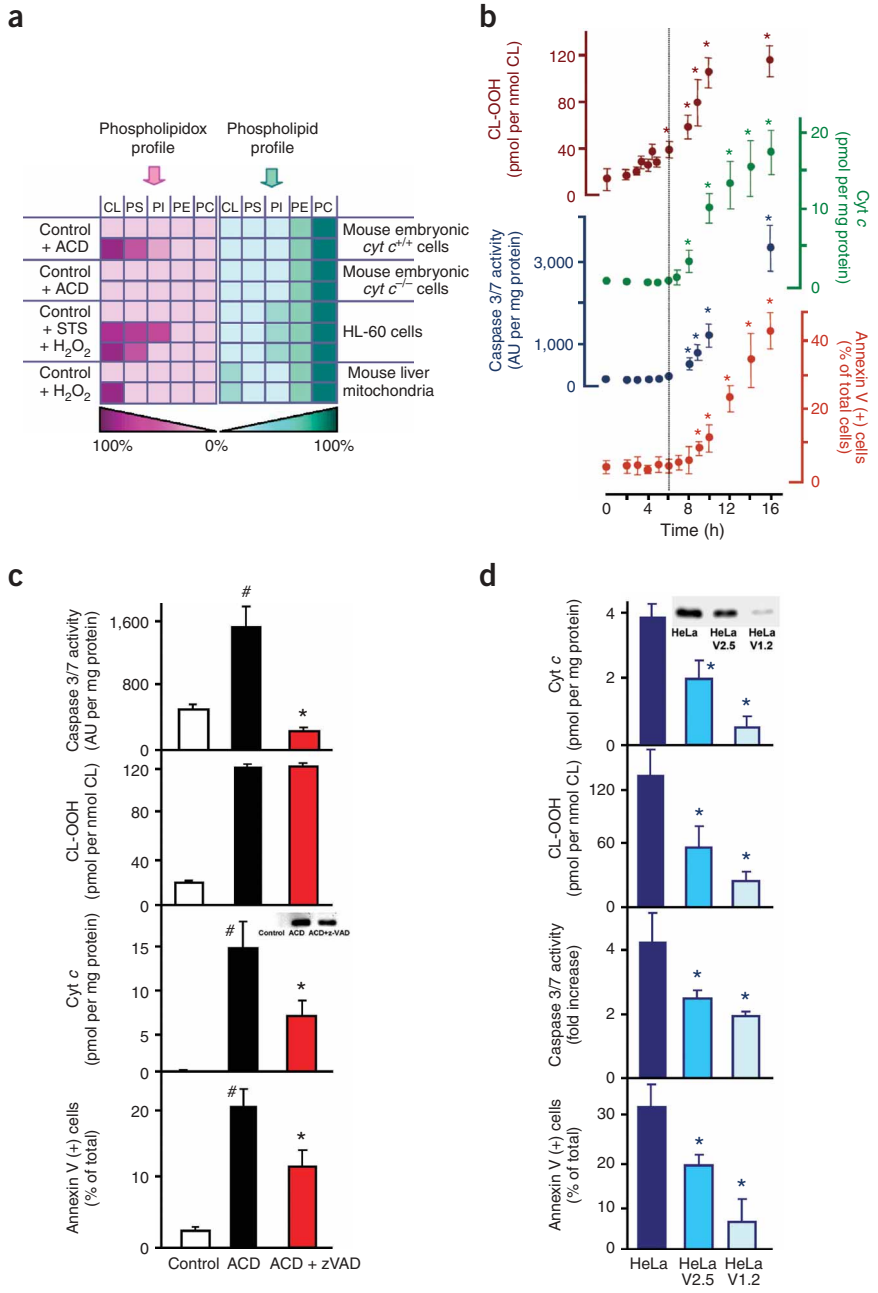

Figure 1 Lipidomics and oxidative lipidomics of apoptosis. (**a**) Profiles of phospholipids and phospholipid hydroperoxides in cells and mitochondria challenged with oxidant or nonoxidant proapoptotic stimuli. Phospholipid content is expressed as percent of total phospholipids and shown in blue-green scale. One hundred percent for mouse embryonic cells and HL-60 cells corresponds to 50 and 40 nmol of phospholipids per 10^6 cells, respectively; for mitochondria, 100% corresponds to 130 nmol of phospholipids per mg protein. Phospholipid hydroperoxides are presented as pmol of phospholipid hydroperoxide per nmol of phospholipid and shown in pink-red scale. One hundred percent corresponds to 140, 100 and 130 pmol of phospholipid hydroperoxides per nmol of specific phospholipid for mouse embryonic cells, HL-60 cells and mitochondria, respectively. (**b**) Time course of biomarkers of apoptosis induced by ACD (100 ng ml^{-1}, for 16 h at 37 °C) in *cyt* $c^{+/+}$ cells. Note that statistically significant accumulation of CL hydroperoxides (dotted line) precedes cyt *c* release, caspase 3/7 activation and PS externalization. Data are means ± s.d., $^*P < 0.05$ versus nontreated cells, $n = 4$. (**c**) Inhibition of caspases 3/7 by a pan-caspase inhibitor, z-VAD-fmk (80 μM), did not affect CL peroxidation but was associated with partial inhibition of cyt *c* release from mitochondria and PS externalization during apoptosis induced by ACD (100 ng ml^{-1}, for 10 h at 37 °C) in *cyt* $c^{+/+}$ cells. Inset: western blots of cyt *c* released into cytosol of control *cyt* $c^{+/+}$ cells and ACD-treated cells in the absence and presence of pan-caspase inhibitor, z-VAD-fmk. Western blots prototypical of three independent experiments are presented. Data are means ± s.d., $^{\#}P < 0.05$ versus control; $^*P < 0.05$ versus ACD-treated *cyt* $c^{+/+}$ cells in the absence of z-VAD-fmk, $n = 4$. (**d**) Content of cyt *c* in HeLa cells and cyt *c* siRNA clones HeLaV1.2 and HeLaV2.5 and biomarkers of apoptosis in them during ACD-induced apoptosis (100 ng ml^{-1} for 10 h at 37 °C). Note that decreased levels of cyt *c* in the clones are associated with their decreased sensitivity to apoptosis. Data are means ± s.d., $n = 4$, $^*P < 0.05$ versus control HeLa cells. Inset: western blots of cyt *c* in HeLa cells. Western blots prototypical of three independent experiments are presented.

Moreover, CL oxidation occurred as one of very early mitochondrial responses to proapoptotic stimuli. In ACD-triggered mouse embryonic cells, CL oxidation (6 h) preceded cyt *c* release (8 h), caspase 3/7 activation (8 h) and PS externalization (9 h) (**Fig. 1b**). Notably, a decrease in mitochondrial membrane potential ($\Delta\Psi$) occurred much later (about 12–14 h after treatment with ACD; data not shown), suggesting that mitochondrial membrane permeability transition (MPT) did not have any substantial role in either CL oxidation or cyt *c* release.

Given that CL oxidation happens before caspase activation, it should be insensitive to caspase inhibitors. Indeed, a pan-caspase inhibitor, z-VAD-fmk (which completely inhibited caspases 3/7), did not affect CL peroxidation induced by ACD in *cyt* $c^{+/+}$ cells, but substantially suppressed cyt *c* release and PS externalization (**Fig. 1c**). This suggests that the generation of CL oxidation products occurs upstream of both cyt *c* release and caspase activation, in line with the time course of different biomarkers of apoptosis and CL oxidation (**Fig. 1b**). Thus, CL oxidation may act as a signal required for the execution of subsequent parts of proapoptotic program.

Cyt *c* catalyzes CL oxidation

Because our previous studies showed that PS oxidation can be catalyzed by the H_2O_2-dependent peroxidase activity of cyt *c*[13], we reasoned that CL oxidation might occur through a similar catalytic mechanism. To test whether cyt *c*–associated peroxidase activity is involved in CL oxidation, we compared ACD-induced CL oxidation in *cyt* $c^{+/+}$ mouse embryonic cells with that in cyt *c*–deficient (*cyt* $c^{-/-}$) cells (**Fig. 1a**). In contrast to *cyt* $c^{+/+}$ cells, *cyt* $c^{-/-}$ cells did not show CL oxidation (**Fig. 1a**).

The lack of cyt *c* in *cyt* $c^{-/-}$ cells may be associated with deficiencies in other redox catalytically active components of mitochondrial

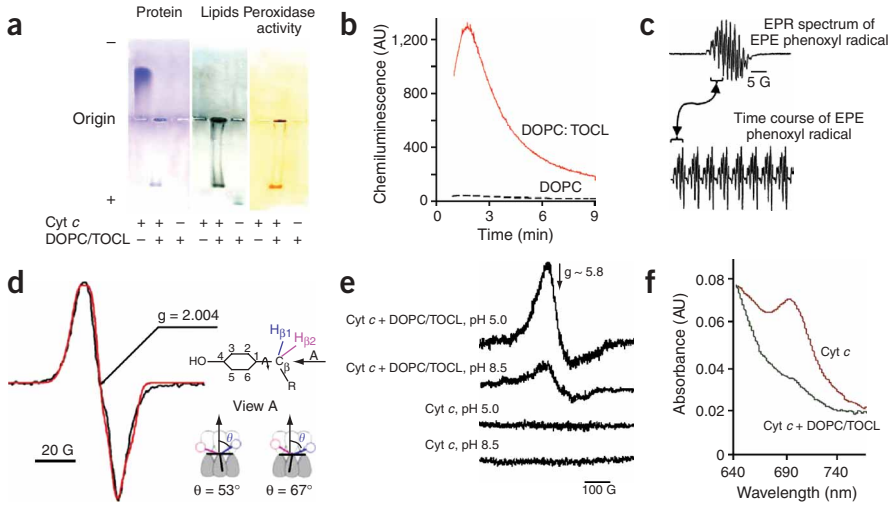

Figure 2 Characterization of peroxidase activity of CL–cyt *c* complexes in model systems. (**a**) Native agarose gel of cyt *c* complexes with TOCL stained for protein, lipids and peroxidase activity. The gel is representative of five independent experiments. (**b**) Assessments of peroxidase activity based on H_2O_2-induced oxidation of luminol to yield a chemiluminescence response. (**c**) EPR-based assessment of cyt *c* peroxidase activity. EPR spectrum and time course of EPE phenoxyl radical generated by TOCL–cyt *c*; a part of the upper spectrum shown by a bracket was scanned repeatedly and presented as a time course. EPR spectra prototypical of six independent experiments are presented. (**d**) Low-temperature EPR spectra of protein-derived radicals of cyt *c*. EPR spectra of protein-derived radical prototypical of five independent experiments are presented. The black trace is the experimental spectrum and the red one is a spectrum simulated by use of the tyrosyl radical EPR spectra simulation algorithm[22] when the input parameters were $\rho_{C1} = 0.41$ and $\theta = 53.0°$. Tyrosine conformation for $\theta = 53.0°$ and spectroscopically identical conformation for $\theta = 67.0°$ are shown for view A, the latter being defined for tyrosine as shown. (**e**) Characterization of Me_{80}-Fe heme interactions in cyt *c* upon binding with DOPC plus TOCL liposomes. Low-field EPR spectrum of cyt *c* in the presence and in the absence of DOPC plus TOCL liposomes in 20 mM sodium-citrate buffer, pH 5.0 and after treatment with chloramine T in 50 mM Tris-HCl buffer, pH 8.5 (77K). (**f**) Absorbance spectra of cyt *c* in the absence and in the presence of DOPC plus TOCL liposomes in 20 mM phosphate buffer pH 7.0, containing DTPA. Spectra prototypical of three independent experiments are presented.

electron transport[14]. Therefore, we tested electron transport activity in *cyt* $c^{-/-}$ cells as compared with *cyt* $c^{+/+}$ cells. Succinate oxidase activity, dependent on electron transport through complexes II, III and IV (ref. 15), was negligible in mitochondria from *cyt* $c^{-/-}$ cells (25 ± 19 mU mg^{-1} protein) compared with those of *cyt* $c^{+/+}$ cells (229 ± 7 mU mg^{-1} protein). However, exogenous cyt *c* reconstituted the activity to essentially the same level in mitochondria from both *cyt* $c^{+/+}$ and *cyt* $c^{-/-}$ cells (335 ± 9 and 318 ± 28 mU mg^{-1} protein, respectively), suggesting that, with the exception of cyt *c*, there were no significant differences between other components of mitochondrial electron transport.

We further used siRNA protocol to generate clones of HeLa cells with significantly differing levels of cyt *c*. Two clones—HeLaV2.5 and HeLaV1.2—were used in which the content of cyt *c* constituted $51.7 \pm 14.0\%$ and $14.0 \pm 7.4\%$, respectively, of its level in parental HeLa cells (100%). Both CL oxidation and sensitivity to ACD-induced apoptosis were proportional to the content of cyt *c* in these cells (**Fig. 1d**).

Execution of apoptosis is accompanied by the mitochondrial generation of superoxide radicals dismutating to H_2O_2 that can be used by catalytically competent CL–cyt c complexes for lipid peroxidation. Importantly, in liver mitochondria isolated from C57BL/J6 mice, H_2O_2 oxidized only CL but not other phospholipids. In HL-60 cells, too, selective oxidation of CL resulted from H_2O_2 treatment (**Fig. 1a**).

We reasoned that enzymatic CL oxidation by cyt *c* during apoptosis should exert different sensitivity to lipid antioxidants than random, nonenzymatic peroxidation of CL in liposomes. Therefore, we used a phenolic lipid radical scavenger, 9-((4,6-*O*-ethylidene-beta-D-glucopyranosyl) oxy) -5,8,8a,9-tetrahydro-5-(4-hydroxy-3,5-dimethoxyphenyl) furo (3′,4′:6,7) naphtha(2,3-d)-1,3 dioxol-6-(5ah)-one (EPE), and found that it was equally effective in inhibiting peroxidation of 1-palmitoyl-2-arachidonoyl phosphatidylcholine (PAPC) and tetra-linoleyl cardiolipin (TLCL) chemically induced in liposomes by an azo-initiator, 2,2′-azobis(2,4-dimethylvaleronitrile) (AMVN, **Supplementary Fig. 1** online). In contrast, oxidation of CL in liposomes induced by cyt *c* plus H_2O_2 exerted only limited sensitivity to EPE (**Supplementary Fig. 1**). Moreover, EPE suppressed oxidation of two major phospholipids, PC and PE, but enhanced oxidation of CL during AMVN-induced apoptosis in HL-60 cells (**Supplementary Fig. 1**). Thus, CL oxidation in liposomes induced by cyt *c* plus H_2O_2 and apoptosis-specific oxidation of CL were selectively insensitive to a radical scavenging activity of a lipid antioxidant, EPE.

CL–cyt *c* complex has peroxidase activity

Compact tertiary structure of solubilized cyt *c*, maintaining hexa-coordinated low-spin configuration of heme iron is prohibitive of its catalytic activation by H_2O_2. Interaction of cyt *c* with anionic lipids induces its folding variant with features of a molten globule state whereby H_2O_2 can get access to the heme catalytic site and trigger the peroxidase activity. To determine the extent to which interactions of cyt *c* with CL might modulate cyt *c* peroxidase activity, we performed agarose gel electrophoresis of cyt *c* alone, tetraoleoyl-CL (TOCL)–cyt *c* complexes and TOCL alone in nondenaturing conditions and stained them for proteins, lipids and peroxidase activity. Binding with TOCL changed the electrophoretic migration profile of cyt *c* such that the complex moved toward the anode (compared to the migration of positively charged cyt *c* to the cathode). The complex stained positively for both lipid content and peroxidase activity (**Fig. 2a**). In independent competition experiments with 10-*N*-nonyl acridine orange (NAO), a positively charged fluorescent molecule with a relatively high affinity for CL[16], we determined binding constants of cyt *c* with CL and confirmed its high affinity for unsaturated CL (**Supplementary Fig. 2** online).

Several types of direct measurements of peroxidase activity using chemiluminescence (**Fig. 2b**), fluorescence (**Supplementary Fig. 3** online) and the electron paramagnetic resonance (EPR) responses (**Fig. 2c**) confirmed that the CL–cyt *c* complex is indeed an active peroxidase; neither cyt *c* alone nor its mixture with dioleoyl-PC (DOPC) liposomes exerted any comparable peroxidase activity.

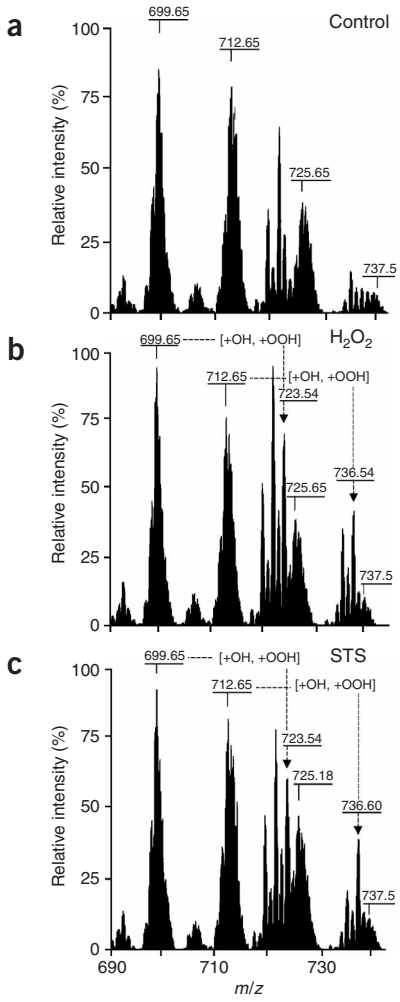

Figure 3 MS analysis of CL oxidation in HL-60 cells. (**a**–**c**) MS-analysis of molecular species of CL in control HL-60 cells (**a**) and CL oxidation during apoptosis induced by oxidant (H_2O_2) (**b**) or nonoxidant (STS) (**c**) treatment. Note the presence of signals from various CL species, that is, with *m/z* 699.6, 712.6, 725.6 and a small amount of 737.3 in nonapoptotic HL-60 cells. On the basis of signal intensity, the abundance of CL molecular species decreased in the order $(C_{16:0})_2(C_{18:2})_2$ (*m/z* 699.6), $(C_{16:0})(C_{18:1})(C_{18:2})_2$ (*m/z* 712.6), $((C_{18:0})(C_{18:1})(C_{18:2})_2)$ (*m/z* 725.6), $((C_{20:0})(C_{18:2})_3)$ (*m/z* 737.3). TLCL (*m/z* 723.5) was not one of the major molecular species in HL-60 cells. Mass spectra prototypical of three independent experiments are presented.

Peroxidase activation of cyt *c* was achieved by unsaturated molecular species of CL (such as TOCL and TLCL), and bovine heart CL (data not shown), whereas saturated CL (tetramyristoyl-CL (TMCL)) was much less efficient at such activation (**Supplementary Fig. 3**).

Catalytic activation of heme peroxidases, such as cyt *c*, involves formation of compound I, the oxoferryl porphyrin π-cation radical[17–19]. One electron reduction of compound I results in transfer of the radical character to an amino acid residue of the protein, in most cases to a tyrosine residue[20,21]. A free radical ($g \sim 2.004$) was formed in the TOCL–cyt *c* complex after addition of H_2O_2 (**Fig. 2d**). The low-temperature EPR signal of this radical was barely detectable in cyt *c* plus H_2O_2 or in a mixture of cyt *c* with DOPC liposomes plus H_2O_2 (data not shown). The overall spectroscopic characteristics of this EPR signal, such as the g-factor (~2.004), the peak-to-trough width (~17 G), the microwave power saturation behavior ($P_{1/2} = 3$ mW, inhomogeneity parameter of 1.6) and a transient character of the radical, all indicated that the radical responsible for the EPR signal was a protein-bound radical, typical of the reaction between many different hemoproteins and peroxides[20,21].

A detailed analysis of the signal's line shape showed that it could be simulated fairly accurately as a tyrosyl radical EPR spectrum when the EPR spectra simulation algorithm suggested for this type of radical[22] was used (**Fig. 2d**). If the radical is indeed on a tyrosine residue of cyt *c*, as the simulation suggests, then the phenoxyl ring rotation angle in such a tyrosyl radical should be either 53.0 ± 2.5° or 67.0 ± 2.5°, the EPR method alone being unable to distinguish between these two possibilities. The relatively high value of the spin density on atom C1 ($\rho_{C1} = 0.41 \pm 0.02$) of the cyt *c* tyrosyl radical, when compared with this parameter of the tyrosyl radicals in other systems, indicates that the tyrosyl radical in cyt *c* might experience a strong hydrogen bond[22].

Using a spin trap, 2-methyl-2-nitrosopropane (MNP) and complexes of cyt *c* with a nonoxidizable TOCL or a highly oxidizable TLCL, we were able to detect either MNP adducts with protein-derived (tyrosyl) radicals or a combination of adducts of protein-derived radicals and lipid radicals, respectively (**Supplementary Fig. 3**). The formation of tyrosyl radicals in peroxidase reactions of the TOCL–cyt *c* complex was confirmed by the formation of dityrosine cross-links resulting in cyt *c* oligomerization (**Supplementary Fig. 3**).

Why does CL complexation induce cyt *c* peroxidase activity? When cyt *c* acts as an electron shuttle between mitochondrial complexes III and IV, all six coordination positions in its heme iron are occupied, thus preventing its interactions with small ligands such as H_2O_2 and NO● (ref. 23). By contrast, cyt *c* bound to mitochondrial CL exerts an entirely different conformation, with partial unfolding of the protein and a weakened or ruptured Fe-Met_{80} bond[24,25]. Nantes and co-authors[26,27] used liquid helium EPR and showed the appearance of a high-spin signal and a modified low-spin signal from cyt *c* upon its interaction with CL-containing membranes, thus indicating weakening and substitution of the Met_{80} ligand. Our EPR experiments at liquid nitrogen temperature also detected a high-spin signal of the TOCL–cyt *c* complex after shifting pH to 5.0 or after treatment of TOCL–cyt *c* complex with chloroamine T at pH 8.5 (that is, chemical modification of Met_{80}; **Fig. 2e**). These high-spin signals of cyt *c* were not observed in the absence of TOCL. In addition, TOCL induced disappearance in cyt *c* absorbance with a maximum at 695 nm ascribed to Met_{80}-heme iron bond[26–28] (**Fig. 2f**), indicating that formation of CL–cyt *c* complex facilitated removal of Met_{80} as a ligand of cyt *c* heme iron. Therefore, interaction of CL with cyt *c* may open up a site for H_2O_2 and small organic peroxides to interact with the heme, conferring catalytic competence on the protein whose peroxidase activity can also function as a specific CL oxygenase. Interestingly, another oxygenase with peroxidase activity, prostaglandin synthase, contains *bis*-histidine hexa-coordinated heme iron[19] and undergoes substantial conformational rearrangements upon binding of arachidonic acid, which undergoes further oxygenation[29].

Mitochondrial pool of cyt *c* selectively oxidizes CL

Next, we used electrospray ionization mass spectrometry (ESI-MS) to determine whether the peroxidase activity of CL–cyt *c* complexes catalyzes oxygenation of CL. In nonapoptotic HL-60 cells, two major signals with *m/z* values of 699.6 and 712.6, corresponding to doubly charged CL species containing $(C_{16:0})_2(C_{18:2})_2$ and $(C_{16:0})(C_{18:1})(C_{18:2})_2$, respectively, were observed, along with less

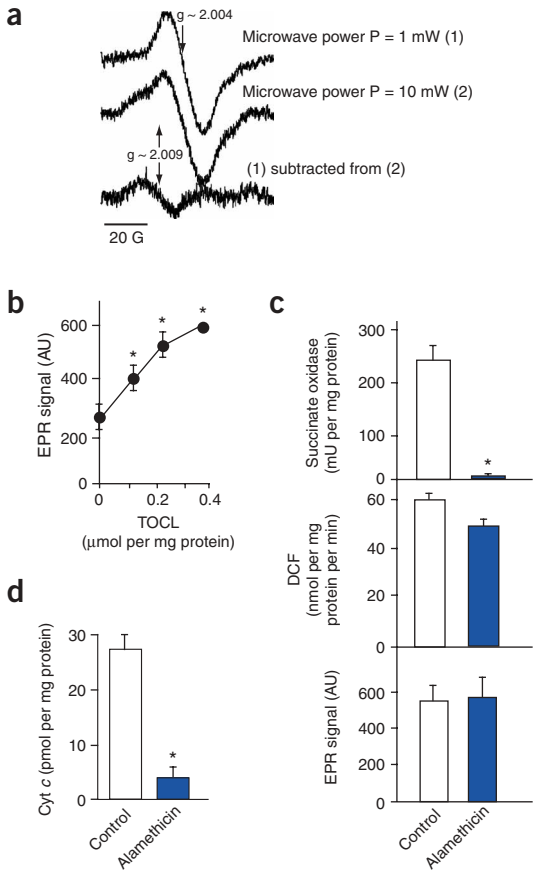

Figure 4 Characterization of peroxidase activity of CL–cyt *c* complex in mitochondria. (**a**) Low-temperature EPR spectra of protein-derived radicals produced in C57BL/6J mouse liver mitochondria in the presence of H_2O_2. EPR spectra of protein-derived radicals prototypical of three independent experiments are presented. (**b**) Effect of TOCL on the magnitude of the EPR signal of protein-derived radicals. Data are means ± s.d., $n = 3$, $^*P < 0.05$ versus control (no TOCL). (**c**) The membrane-permeabilizing antibiotic, alamethicin, inhibits succinate oxidase activity of mouse liver mitochondria but does not significantly affect peroxidase activity of cyt *c* measured by $DCFH_2$ oxidation and EPR signals of protein-derived radicals. (**d**) Alamethicin depletes cyt *c*.

robust signals with *m/z* values of 725.6 ($(C_{18:0})(C_{18:1})(C_{18:2})_2$) and a small amount of 737.3 ($(C_{20:0})(C_{18:2})_3$; **Fig. 3a**). Two abundant CL species containing $C_{18:2}$ acyls underwent oxidation during oxidant (H_2O_2)- (**Fig. 3b**) or nonoxidant (STS)-induced apoptosis (**Fig. 3c**), resulting in signals with *m/z* of 723.54 (*m/z* 699.6 + 8 +16 = *m/z* 723.6) and 736.60 (*m/z* 712.6 + 8 +16 = *m/z* 736.6; **Fig. 3b**,**c**).

TOCL—containing monounsaturated oleic acid residues—is not oxidizable by cyt *c* plus H_2O_2, in sharp contrast to TLCL, which is effectively peroxidized (**Supplementary Fig. 4** online). Therefore, in looking at the reaction *in vitro*, we used TLCL, the most abundant CL molecular species in mitochondria[30], as a reactive substrate. When the TLCL–cyt *c* complex or C57BL/6J mouse liver mitochondria (**Supplementary Fig. 4**) were incubated with H_2O_2, several oxygenated species of CL, including those containing mono-, di-, and trihydroperoxides of CL and its hydroxy derivatives, were detected.

If complexes of cyt *c* with unsaturated molecular species of CL function as peroxidases, their activity should be detectable in mitochondria. Indeed, liquid nitrogen temperature EPR spectroscopy revealed H_2O_2-dependent signal(s) from C57BL/6J mouse liver mitochondria (**Fig. 4a**). Two overlapping components were immediately discernable in the spectra of H_2O_2-treated mitochondria. The central component had characteristics very close to those of the TOCL–cyt *c* EPR signal (g ~ 2.004 and peak-to-trough width of ~21 G) and included signals from two species as evidenced by power saturation behavior (**Fig. 4a**). The second component, observed as a low-field shoulder (g ~ 2.01), can be tentatively assigned to a peroxyl radical[31]; however, the lack of a weak peak at g = 2.036, which could not be detected at the present signal-to-noise ratio, precluded an unambiguous conclusion. The appearance of protein-derived radicals in H_2O_2-treated mitochondria was further supported by MNP spin-trapping (**Supplementary Fig. 5** online). Moreover, we were able to detect substantial peroxidase activity in C57BL/6J mouse liver mitochondria as evidenced by H_2O_2-dependent oxidation of 2′,7′-dichlorodihydrofluorescein ($DCFH_2$, **Supplementary Fig. 5**). The peroxidase activity in mitochondria obtained from *cyt* $c^{+/+}$ mouse embryonic cells was markedly higher than in mitochondria from *cyt* $c^{-/-}$ cells (**Supplementary Fig. 5**). These observations and the fact that addition of CL to mitochondria increased the magnitude of the H_2O_2-induced low-temperature EPR signal (**Fig. 4b**) support that mitochondrial cyt *c* contributes to the EPR signals observed.

These results raise the question of how the peroxidase function of cyt *c* interrelates with its major role as an electron transporter between

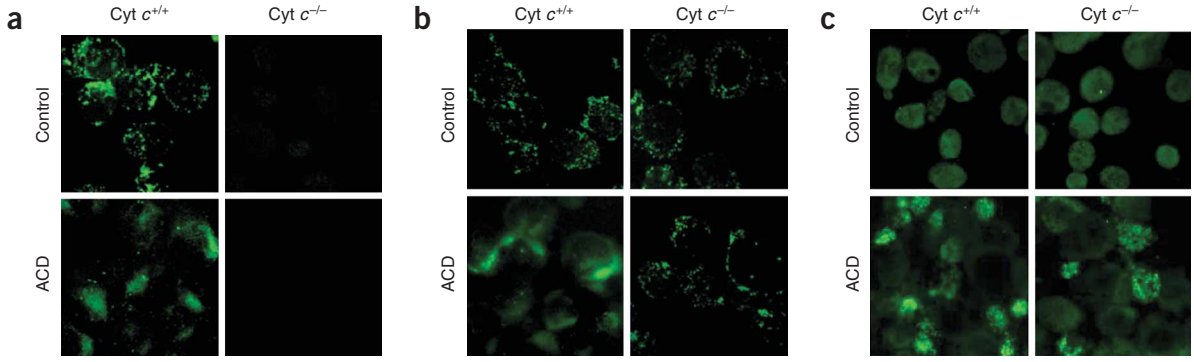

Figure 5 Cyt *c*–catalyzed oxidation of CL is required for release of proapoptotic factors from mitochondria into the cytosol of cells during apoptosis. (**a**–**c**) Immunofluorescence staining of cyt *c* (**a**), Smac/Diablo (**b**) and Bax (**c**) in *cyt* $c^{+/+}$ and *cyt* $c^{-/-}$ cells before and after treatment with ACD (100 ng ml^{-1}, for 16 h at 37 °C). Note that release of proapoptotic factors was detectable in *cyt* $c^{+/+}$ but not in *cyt* $c^{-/-}$ cells. Photomicrograph is representative of three experiments.

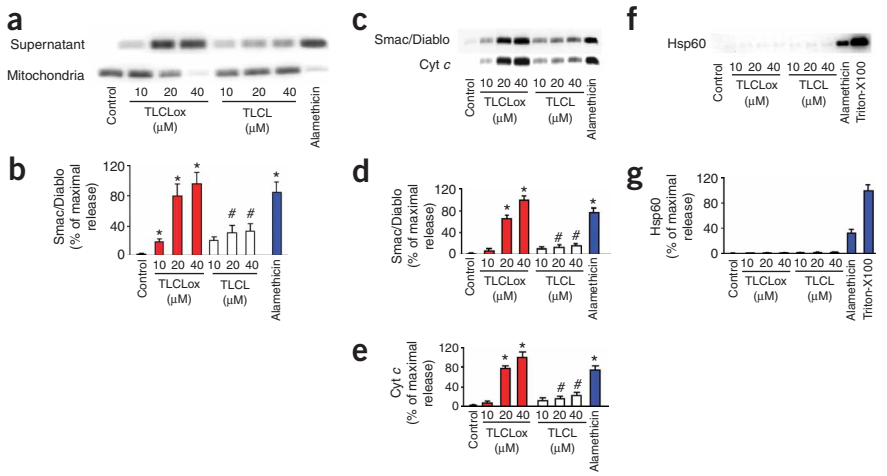

Figure 6 Oxidized cardiolipin (TLCLox) effectively releases Smac/Diablo from mitochondria isolated from *cyt* $c^{-/-}$ mouse embryonic cells as well as cyt *c* and Smac/Diablo from mitochondria of *cyt* $c^{+/+}$ cells. (**a**–**g**) Smac/Diablo in *cyt* $c^{-/-}$ mitochondria (**a**,**b**), Smac/Diablo and cyt *c* (**c**–**e**) and Hsp60 (**f**,**g**) in *cyt* $c^{+/+}$ mitochondria were examined by western blots and the amounts of proteins released into cytosol or remaining in mitochondria estimated by densitometry. Data are means ± s.d., $n = 3$, $^{*}P < 0.05$ versus control, $^{\#}P < 0.05$ versus TLCL.

mitochondrial complexes III and IV (ref. 32). To address this, we performed measurements of peroxidase activity and electron-transport (succinate oxidase) activity in liver mitochondria before and after treatment with alamethicin, known to permeabilize mitochondrial membranes and remodel cristae to remove loosely (electrostatically) bound cyt *c* from mitochondria (in contrast to digitonin, which only permeabilizes the outer mitochondrial membrane and releases 15–20% of total cyt *c*[6,33]). The results showed that alamethicin caused almost complete inhibition of succinate oxidase activity without affecting the peroxidase activity (**Fig. 4c**). This effect of alamethicin was accompanied by a removal of most (~85%) but not all cyt *c* from mitochondria, in line with the previously published data[34–36]. Still, about 15% of total cyt *c* remained in mitochondria, likely in a form bound to CL[6] (**Fig. 4d**). The electron transport activity of mitochondrial suspensions could be fully restored by adding exogenous cyt *c*. However, when CL was added along with cyt *c*, restoration of succinate oxidase activity was incomplete and dependent on the amount of CL (**Supplementary Fig. 5**).

Release of proapoptotic factors by CL oxidation products

We next sought to assess the importance of CL–cyt *c* complexes in CL oxidation and release of proapoptotic factors from mitochondria. Thus, we challenged *cyt* $c^{+/+}$ and *cyt* $c^{-/-}$ cells with ACD. Release of cyt *c* was detected in apoptotic *cyt* $c^{+/+}$ cells but could not be assessed in *cyt* $c^{-/-}$ cells (**Fig. 5a**). Therefore, we used Smac/Diablo as another proapoptotic marker released from mitochondria during apoptosis. In *cyt* $c^{+/+}$ cells, immunofluorescence of both cyt *c* and Smac/Diablo revealed a typical punctate pattern of their mitochondrial distribution in control that changed to a more even cytosolic pattern of distribution after treatment with ACD (**Fig. 5b**). In *cyt* $c^{-/-}$ cells, however, stimulation with ACD did not affect distribution of Smac/Diablo. Using western blots, we established that ACD effectively induced release of Smac/Diablo in *cyt* $c^{+/+}$ cells; exposure of *cyt* $c^{-/-}$ cells to ACD did not induce any considerable release of Smac/Diablo, which remained confined to the mitochondrial pellet (**Supplementary Fig. 6** online). Accordingly, ACD did not induce other apoptotic biomarkers such as PS externalization and nuclear fragmentation in *cyt* $c^{-/-}$ cells (data not shown). The failure of *cyt* $c^{-/-}$ cells to release proapoptotic factors after ACD stimulation was not due to deficiency in Bax-dependent mechanisms, as control experiments with immunofluorescence staining (**Fig. 5c**) and western blotting (**Supplementary Fig. 6** online) showed that Bax was translocated from the cytosol into mitochondria after ACD treatment in both *cyt* $c^{+/+}$ and *cyt* $c^{-/-}$ cells.

The inability of *cyt* $c^{-/-}$ cells to release proapoptotic factors during apoptosis could be overridden by the addition of oxidized CL to *cyt* $c^{-/-}$ mitochondria. We prepared oxidized TLCL (TLCLox) by incubating TLCL and cyt *c* in the presence of H_2O_2 to mimic the conditions of CL oxidation via the peroxidase activity of the CL–cyt *c* complex in mitochondria during apoptosis. TLCLox was effective in concentration-dependent release of Smac/Diablo from the mitochondria of *cyt* $c^{-/-}$ cells, whereas nonoxidized TLCL showed only slight activity in releasing proapoptotic factors (**Fig. 6a**,**b**). Similarly, TLCLox (but not nonoxidized TLCL) caused a concentration-dependent release of both Smac/Diablo and cyt *c* from the mitochondria of *cyt* $c^{+/+}$ cells (**Fig. 6c**–**e**). To test the specificity of TLCLox action, we determined the extent to which TLCLox was able to induce release of a matrix protein, Hsp60, from mitochondria of *cyt* $c^{+/+}$ cells. We found that only trace amounts of Hsp60 were detectable in the supernatant fraction after treatment of mitochondria with either TLCL or TLCLox. In contrast, alamethicin, a membrane-permeabilizing antibiotic, effectively released substantial amounts of Hsp60 (**Fig. 6f**,**g**). Moreover, treatment of mitochondria with a nonionic detergent, Triton X-100, resulted in almost complete release of Hsp60 from the mitochondrial matrix (**Fig. 6f**,**g**). Thus, TLCLox induced specific release of proapoptotic factors from the intermembrane space of mitochondria, rather than acting nonspecifically in a detergent-like manner. As Smac/Diablo is not known to act as a CL-binding protein, CL oxidation seems to be involved in both an increase in the pool of cyt *c* available for the release[6] and mitochondrial outer membrane permeabilization.

CL availability, unsaturation and apoptosis

CL is found almost exclusively in the inner mitochondrial membrane, where it accounts for 25% of all phospholipids[37]; a substantial part of total CL is confined to the matrix side of the membrane[38]. On the basis of the availability of CL to phospholipase A_2, we estimated that less than 5 mol% of CL was detectable in the outer mitochondrial membrane of nonapoptotic HL-60 cells (**Fig. 7a**). CL distribution between the matrix and intermembrane surfaces of the inner mitochondrial membrane was 60:40, in agreement with previously published results[39,40]. In apoptotic STS-triggered HL-60 cells, however, the CL content in the outer mitochondrial membrane markedly increased to reach a level of approximately 40 mol%. The CL distribution between the two monolayers of the inner membrane also changed, such that almost 70 mol% of CL was detectable in the outer monolayer, whereas 30 mol% was confined to the matrix side of the membrane (**Fig. 7b**). According to a previous study[39], the inter- and intramembrane translocations of CL occur very early during

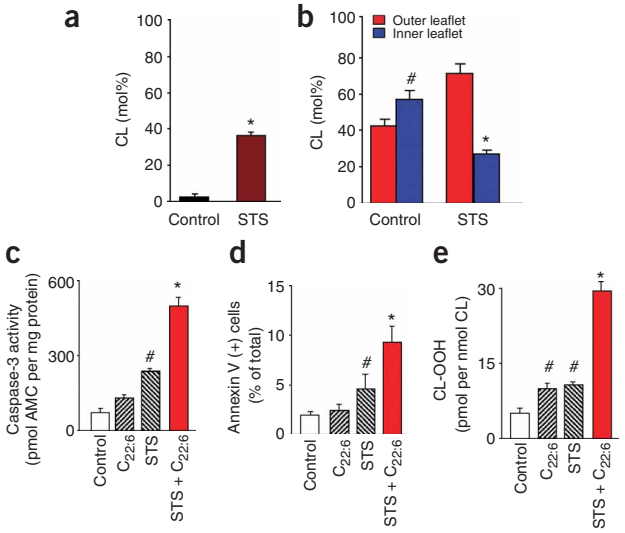

Figure 7 Distribution of CL in mitochondrial membranes and effects of CL unsaturation on STS-triggered apoptosis in HL-60. Content of CL in the outer and inner mitochondrial membranes of nonapoptotic HL-60 cells and after STS-induced apoptosis. (**a**) Outer mitochondrial membrane and (**b**) inner and outer leaflets of mitoplasts isolated from control and STS-treated HL60 cells. Note that STS caused a notable increase of CL in the outer mitochondrial membrane and CL redistribution between the matrix surface and intermembrane surface in the inner membrane. Data are means ± s.d., $^{\#,*}P < 0.05$ versus control, $n = 3$. HL-60 cells enriched with $C_{22:6}$-containing CL molecular species showed greater CL oxidation and increased sensitivity to STS-triggered apoptosis. (**c**) Caspase-3 activation, (**d**) PS externalization and (**e**) CL oxidation. Data are means ± s.d., $n = 3$, $^{\#}P < 0.05$ versus control, $^{*}P < 0.05$ versus $C_{22:6}$ or STS.

apoptosis—well before changes in mitochondrial membrane potential or other markers of apoptosis, such as plasma-membrane exposure of PS, but after the production of reactive oxygen species (ROS)[39]. Thus, the amounts of CL that may become available for interactions with cyt *c*, and hence for tight binding of cyt *c* in the membrane, change substantially during apoptosis. Although there is ~70-fold excess of CL available for 1:1 stoichiometric binding with cyt *c*[30,38], most CL is not free but rather interacts with essentially all mitochondrial electron-transporting complexes[41]. In addition, apoptosis-associated proteins such as Bid and tBid have CL-binding domains[42] and compete with cyt *c* for CL (**Supplementary Fig. 7** online). Obviously, CL's role and participation in outer membrane permeabilization should be considered in lieu of the different affinities of CL toward these CL-binding proteins.

If both cyt *c* and CL are essential components of the catalytic complex that is ultimately involved in the formation of CLox and its subsequent participation in the execution of the apoptotic program, then enrichment of cells with CL molecular species more readily susceptible to peroxidation should facilitate apoptosis. By growing HL-60 cells in the presence of $C_{22:6}$, we were able to enrich them with CL molecular species containing highly oxidizable $C_{22:6}$. MS analysis revealed the presence of new, relatively abundant CL molecular species containing $C_{22:6}$ with singly charged MS signals of *m/z* 1648 and 1656 corresponding to $(C_{22:4})_1(C_{22:5})_1(C_{22:6})_2$ and $(C_{22:0})_1(C_{22:5})_1(C_{22:6})_2$, respectively. Accordingly, a higher level of CL oxidation correlated with a higher sensitivity to STS-induced apoptosis in $C_{22:6}$-enriched HL-60 cells versus HL-60 cells grown in standard conditions (**Fig. 7c–e**).

DISCUSSION

The apoptotic program relies heavily on protein-protein interactions that regulate it at different levels. Susceptibility to cell death and execution of the death program involve several critical protein-protein interactions between different anti- and proapoptotic members of the Bcl-2 family, between cyt *c* and Apaf-1 during apoptosome formation, and between IAPs and caspases. Disruptors of these protein-protein interactions have been successfully used for new targeted therapeutic approaches[43]. This report shows, for the first time, that lipid-protein interactions between CL and cyt *c* are also critical for the execution of the apoptotic program. A seminal work[4] established that permeabilization of the outer mitochondrial membrane through interactions of Bcl-2 family proteins (Bax and Bid) resulting in the release of proapoptotic factors had an absolute requirement for CL. However, neither prerequisite molecular features of CL (for example, their fatty acid composition) nor modified forms of CL (peroxidized or partially hydrolyzed to lyso-CL) have been identified as essential for the permeabilizing activity. Subsequent work in this area revealed that Bcl-2 proteins, particularly Bid or tBid and Bax, had dynamic interactions with CL metabolites, especially molecular species of lyso-CL such as mono- and di-lyso-CL (reviewed in ref. 44). These interactions between CL and Bcl-2 proteins are likely to be mostly effective at the contact sites of the inner and outer mitochondrial membranes, resulting in the reorganization of CL in microdomains with a hexagonal H_{II} configuration favorable for the release of proapoptotic factors[45]. The role of oxidatively modified CL in mitochondrial membrane permeabilization has not been investigated. Our results show that oxidized CL was essential for the release of proapoptotic factors from mitochondria into the cytosol, whereas nonoxidized CL was markedly less efficient. It is possible that the effect of CLox was realized through its association with Bcl-2 family proteins such as Bax and Bid. Our data also show that cyt *c* has a markedly higher (approximately two orders of magnitude) affinity for nonoxidized CL than tBid. Given also that cyt *c* concentrations in mitochondria are an order of magnitude higher than those of Bid[46], one may wonder how an association and subsequent effects of CL on Bcl-2 proteins can be realized. In this regard, important data[30,47] show a substantially reduced binding of CL hydroperoxides (as compared with nonoxidized CL) with cyt *c*. On the basis of both this and our results that cyt *c* acts as a catalyst of CL oxidation and CLox is essential for the release of proapoptotic factors from mitochondria, it is tempting to speculate that interactions of CLox rather than of CL with Bcl-2 family proteins participate in permeabilization of the outer mitochondrial membrane. In this model, cyt *c*–catalyzed CL oxidation is a necessary step preceding interactions of CLox with Bcl-2 family proteins in the chain of events leading to the release of cyt *c* from mitochondria. Our results are compatible with the two-stage model for cyt *c* release from mitochondria, whereby CL oxidation is required for both cyt *c* detachment from the inner mitochondrial membrane and for permeabilization of the outer membrane followed by the release of cyt *c* into the cytosol[6].

Permeabilization of the outer mitochondrial membrane and release of proapoptotic factors from mitochondria regulated by Bcl-2 family proteins do not seem to require the obligatory MPT. In fact, two recent papers[48,49] have clearly shown that cyclophilin D–dependent MPT does not have any important role in apoptosis. In *cyt* $c^{+/+}$ mouse embryonic cells triggered with ACD, $\Delta\Psi$ changes occurred much later than CL oxidation, cyt *c* release, caspase activation and PS externalization. This suggests that MPT was not likely to have a role in CL oxidation and cyt *c* release.

Thus, participation of cyt *c* in apoptosis begins much earlier than suggested by its well-recognized role in the formation of apoptosomes and caspase activation. Mitochondria contain a pool of cyt *c*, which, through interactions with CL, acts as a CL oxygenase that is activated during apoptosis and causes oxidation of CL, which is required for the release of proapoptotic factors. It has been known for more than a decade that dispatch of the apoptotic program is accompanied by early mitochondrial production of ROS[50]. Because antioxidant supplementation and overexpression of antioxidant enzymes protect cells against apoptosis induced not only by pro-oxidant stimuli but also by nonoxidant proapoptogens[51,52], it seems logical that ROS production is not likely to be a meaningless side effect of mitochondrial disintegration but rather an important feature of the apoptotic program. The specific nature of this role is not yet understood. Our current data indicate that cyt *c* uses the generation of oxidizing equivalents to facilitate selective oxidation of CL and, hence, to initiate permeabilization of the outer mitochondrial membrane and subsequent release of proapoptotic factors from mitochondria. Thus ROS production during apoptosis is not an unavoidable side effect but an important signaling pathway realized through its interactions with the CL–cyt *c* complex.

It is likely that, under usual circumstances, the peroxidase function of the CL–cyt *c* complex is that of an antioxidant, protective enzyme helping to remove excess H_2O_2. Our estimates indicate that the peroxidase activity of the CL–cyt *c* complex can be as high as 200 M^{-1} s^{-1} and is readily detectable at H_2O_2 levels as low as 5–10 μM. This suggests that the peroxidase activity of CL–cyt *c* may favorably compete with other mitochondrial and peroxisomal H_2O_2-scavenging enzymes (GSH peroxidase IV, peroxyredoxins, catalase) to control H_2O_2 levels at the expense of intracellular reductants, particularly ascorbate. Production of H_2O_2 during apoptosis changes the role of the CL–cyt *c* complex: depletion of endogenous reductants allows the peroxidase to use CL as the preferential oxidation substrate, generating a new signal—an oxidized molecular species of CL, whose accumulation triggers release of proapoptotic factors from mitochondria. Thus, interactions of cyt *c* with CL govern cyt *c*'s functions in mitochondria and determine its redistribution between two pools: electron carrier and peroxidase.

METHODS

Cells. HL-60 cells (ATCC) were cultured in RPMI 1640 medium supplemented with 15% FBS. Mouse embryonic *cyt* $c^{-/-}$ cells (ATCC) and *cyt* $c^{+/+}$ cells (courtesy of X. Wang, University of Texas, Dallas) were cultured in DMEM supplemented with 15% FBS, 25 mM HEPES, 50 mg l^{-1} uridine, 110 mg l^{-1} pyruvate, 2 mM glutamine, 1× nonessential amino acids, 2′-mercaptoethanol, 0.5×10^6 U l^{-1} mouse leukemia inhibitory factor, 100 U ml^{-1} penicillin and 100 μg ml^{-1} streptomycin. HeLa cells were cultured in the same conditioned medium as mouse embryonic cells but without leukemia inhibitory factor. Cyt *c* siRNA plasmids (target sequences: V1, AAGAAGTACATCCCTGGAACA, and V2, AAGCACAAGACTGGGCCAAAT) were constructed with the pSEC hygro vector (Ambion) and introduced into HeLa cells with liposomes FuGENE 6 (Roche Diagnostic Co.).

Protein, lipids and peroxidase activity of CL–cyt *c* complexes. After agarose gel electrophoresis in 35 mM HEPES buffer pH 7.4 containing 43 mM imidazole, protein, lipids and peroxidase activity of the CL–cyt *c* complexes were revealed by Coomassie Blue R-250, Sudan Black B, and 3,3′-diaminobenzidine, respectively. Cyt *c* (120 μM) and DOPC plus TOCL liposomes (2.4 mM at a ratio of 1:1) were incubated in 50 mM phosphate buffer (pH 7.4) containing DTPA before application onto 0.8% agarose gel. The images were analyzed with the Bio-Rad Multi-Analysis Software.

EPR spectroscopy of CL–cyt *c* peroxidase intermediates. All EPR spectra were recorded on a JEOL-RE1X EPR spectrometer. Spin-trapped MNP radical adducts with protein- and lipid-derived radicals were determined as previously described[53,54]. Cyt *c* (0.5 mM) was incubated with DOPC plus CL liposomes (10 mM at a ratio of 1:1) in the presence of MNP (20 mM) and H_2O_2 (2 mM) in 20 mM phosphate buffer pH 7.4 containing DTPA. EPR spectra were recorded 7 min after H_2O_2 addition. EPR conditions: 3,350 G center field; 100 G sweep width; 2 G field modulation; 20 mW microwave power; 0.3 s time constant; 4 min scan time; and 2.5×10^3 and 5×10^3 receiver gain for liposomes and mitochondria, respectively (two spectra were averaged for extracted lipid radical adducts). To confirm the formation of protein-derived radical, samples were treated with pronase Type XIV (2 mg ml^{-1}) as described[54]. Liquid nitrogen (77K) EPR spectra of high-spin iron in CL–cyt *c* complexes were recorded at 1,100 G center field; 500 G sweep width, 10 G field modulation; 0.3 s time constant; 8 min scan time; 5×10^2 receiver gain; and 5 mW microwave power. Cyt *c* (1 mM) was incubated with DOPC plus TOCL liposomes (50 mM) in the presence of H_2O_2 (2 mM) in 10 mM HEPES pH 7.0 containing DTPA. EPR spectra of protein-derived radicals (at 77K) were recorded at 100 G sweep width; 1 G field modulation; 4 mW microwave power; 0.1 s time constant; and 4 min scan time. Protein-bound EPR spectrum simulation was performed by Simpow6 (M. Nilges, Illinois EPR Research Center, http://ierc.scs.uiuc.edu/~nilges/software.html), when the input parameters were determined by the tyrosyl radical EPR spectra simulation algorithm[22].

Peroxidase activity of CL–cyt *c* complexes. Peroxidase activity was determined by measurement of the following: (i) Fluorescence of 2′,7′-dichlorofluorescin, an oxidation product of 2′,7-dichlorodihydrofluorescein ($DCFH_2$) (λ_{ex} 502 nm, λ_{em} 522 nm), $DCFH_2$ was prepared from $DCFH_2$-DA[13]. Conditions: cyt *c* (2 μM); liposomes (100 μM at a ratio of 1:1); $DCFH_2$ (10 μM); 25 mM HEPES containing DTPA, pH 7.0. (ii) Fluorescence of resorufin, an oxidation product of *N*-acetyl-3,7-dihydroxyphenoxazine (Amplex Red (Molecular Probes); λ_{ex} 570 nm, λ_{em} 585 nm) with a Shimadzu RF-5301PC spectrofluorophotometer. Conditions: cyt *c* (0.01 μM); liposomes (0.2 μM at a ratio of 1:1); H_2O_2 (10 μM); Amplex Red (50 μM); 25 mM HEPES containing DTPA, pH 7.0. (iii) Chemiluminescence of luminol with a LKB-1251 chemiluminometer (LKB-Pharmacia). Conditions: cyt *c* (10 μM); DOPC plus TOCL (100 μM at a ratio of 1:1) or DOPC (100 μM); H_2O_2 (100 μM); luminol (500 μM); 10 mM phosphate buffer; pH 7.4. (iv) EPR spectroscopy of EPE phenoxyl radical produced by oxidation of EPE at 25 °C. Samples (50 μl) contained DOPC plus CL liposomes (250 μM at a ratio of 1:1), cyt *c* (40 μM), EPE (700 μM), and H_2O_2 (100 μM). The EPR conditions were as follows: 3,350 G center field; 0.4 G field modulation; 10 mW microwave power; 0.1 s time constant; 4,000 receiver gain; and 4 min time scan. The kinetics of EPE phenoxyl radical formation was measured by repeated scanning of an indicated part of its EPR signal as shown in **Figure 2c**.

Activity of succinate oxidase. This was assessed by a coupled assay using fumarase and malic dehydrogenase reactions to oxidize fumarate and reduce NAD to NADH in the presence or absence of cyt *c* (10 μM). Even in the presence of an excess of oxidized cyt *c*, the major part of electron flow goes from complex II to oxygen if the incubation medium does not contain KCN[36].

Oxidative lipidomics. *Cyt* $c^{-/-}$ and *cyt* $c^{+/+}$ mouse embryonic cells were exposed to ACD (100 ng ml^{-1}) for 16 h at 37 °C. HL-60 cells (10^6 cells per ml) were treated with either H_2O_2 (25 μM, four times every 30 min) for 2 h at 37 °C or STS (1 μM) for 3 h, 37 °C. Mitochondria (1 mg protein per ml) were exposed to H_2O_2 (50 μM, six times every 10 min) for 1 h at 37 °C. Lipids were extracted from cells and resolved by 2D HPTLC as previously described[55]. Spots of phospholipids were scraped from the HPTLC plates and phospholipids were extracted from silica. Lipid phosphorus was determined by a micro-method[55]. Oxidized phospholipids were hydrolyzed by pancreatic phospholipase A_2 (2 U μl^{-1}) in 25 mM phosphate buffer containing 1 mM $CaCl_2$, 0.5 mM EDTA and 0.5 mM SDS (pH 8.0 at room temperature for 30 min). Fatty acid hydroperoxides formed were determined by fluorescence HPLC of resorufin stoichiometrically formed during their microperoxidase 11–catalyzed reduction in the presence of Amplex Red for 40 min at 4 °C (V. Ritov, V. Tyurin, Y. Tyurina and V. Kagan, *Toxicol. Sci.*, **78**, 114, 2004). Fluorescence HPLC (Eclipse XDB-C18 column, 5 μm, 150 × 4.6 mm, mobile phase

composed of 25 mM disodium phosphate buffer (pH 7.0)/methanol (60:40 v/v), excitation = 560 nm, emission = 590 nm) was performed on a Shimadzu LC-100AT HPLC system equipped with a fluorescence detector (RF-10Axl) and autosampler (SIL-10AD). DOPC plus TLCL (500 μM, at a ratio of 1:1) or DOPC plus TOCL (500 μM, at a ratio of 1:1) liposomes were oxidized by incubation in the presence of cyt *c* (20 μM) and H_2O_2 (100 μM, four times every 15 min) for 60 min at 37 °C in 50 mM phosphate buffer containing 100 μM DTPA at pH 7.4. At the end of incubation, lipids were extracted and hydroperoxides of CL were determined by fluorescence HPLC using the Amplex Red protocol.

ESI tandem MS. ESI-MS of TLCL oxidation products and CL extracted from cells or mitochondria was performed by direct infusion into a triple quadrupole mass spectrometer (Micromass, Inc.). Sheath flow was adjusted to 5 μl min^{-1} and the solvent consisted of chloroform/methanol (1:2, v/v). The electrospray probe was operated at a voltage differential of −3.5 keV in the negative ion mode. Mass spectra for doubly and singly charged CL were obtained by scanning in the range of 400–950 and 1,200–1,800 *m/z*, respectively, every 1–1.5 s and summing individual spectra. Source temperature was maintained at 70 °C. Collision-induced association spectra were obtained by selection of the ion of interest and performance of daughter ion scanning in Q3 at 400 *m/z* with Ar as the collision gas.

Membrane distribution of CL. The membrane distribution of CL in mitochondria and mitoplasts isolated from normal and apoptotic HL-60 cells was determined by monitoring of CL hydrolysis after treatment with porcine pancreatic phospholipase A_2 (60 min at 0–4 °C). To avoid nonspecific interactions of phospholipase A_2 with CL, bovine serum albumin was used as described[56].

Biomarkers of apoptosis. Release of Smac/Diablo and cyt *c* and activation of Bax were estimated by western blotting. Mitochondria and cytosolic fractions were subjected to 12% SDS-PAGE and then transferred to a nitrocellulose membrane, which was probed with anti-cyt *c* (clone 7H8.2C12), anti-Smac/Diablo (clone 7) or anti-Bax (clone 6A7) antibody (Pharmingen) followed by horseradish peroxidase–coupled detection. For immunofluorescence analysis, cells were fixed with 4% paraformaldehyde and permeabilized in PBS containing 0.2% Triton X-100. After 30-min blocking with 2% of BSA in PBS, samples were incubated with anti-cyt *c* (clone 6H2.B4, Pharmingen), anti-Smac/Diablo or anti-Bax antibody followed by FITC-conjugated goat anti-mouse IgG antibody (Upstate). Apoptotic nuclear morphology was determined by staining with Hoechst 33342 (1 μg ml^{-1}) and examination by fluorescent microscopy. Results were expressed as the percentage of cells showing characteristic nuclear morphological features of apoptosis (nuclear condensation and fragmentation) relative to the total number of counted cells (>300 cells). Caspase-3/7 activity was measured with a luminescence Caspase-Glo™ 3/7 assay kit (Promega). PS externalization was determined with the Annexin V-FITC Apoptosis Detection Kit (BioVision, Mountain View, CA).

Additional methods. The following methods can be found in **Supplementary Methods** online: isolation of mitochondria and mitoplasts, preparation of liposomes, binding constants, the intactness of Met_{80} distal ligand, formation of dityrosine crosslinks, the effect of tBid on peroxidase activity TOCL/cyt *c* complex, hydrogen peroxide, mitochondrial membrane potential, statistics, protein-derived radicals in mitochondria, enrichment of CL in HL-60 cells with $C_{22:6}$ preparation of TLCL and treatment of mitochondria, characterization of Me_{80}–Fe heme interactions in cyt *c* upon binding with DOPC plus TOCL liposomes.

Accession codes. BIND identifiers (http://bind.ca/): 315503, 315504.

Note: Supplementary information is available on the Nature Chemical Biology website.

ACKNOWLEDGMENTS
This work was supported by the US National Institutes of Health (grants 1RO1 HL70755 and PO1 HL070807), the US National Insitute for Occupational Safety and Health (grant 1RO1 OH008282) and the International Human Frontier Science Program.

COMPETING INTERESTS STATEMENT
The authors declare that they have no competing financial interests.

Received 23 March; accepted 19 July 2005
Published online at http://www.nature.com/naturechemicalbiology/

1. Green, D.R. & Kroemer, G. The pathophysiology of mitochondrial cell death. *Science* **305**, 626–629 (2004).
2. Kroemer, G. & Reed, J.C. Mitochondrial control of cell death. Targeting of tBid. *Nat. Med.* **6**, 513–519 (2000).
3. Lutter, M. *et al.* Cardiolipin provides specificity for targeting of tBid to mitochondria. *Nat. Cell Biol.* **2**, 754–761 (2000).
4. Kuwana, T. *et al.* Bid, Bax, and lipids cooperate to form supramolecular openings in the outer mitochondrial membrane. *Cell* **111**, 331–342 (2002).
5. Iverson, S. & Orrenius, S. The cardiolipin-cytochrome c interaction and the mitochondrial regulation of apoptosis. *Arch. Biochem. Biophys.* **423**, 37–46 (2004).
6. Ott, M., Robertson, J., Gogvadze, V., Zhivotovsky, B. & Orrenius, S. Cytochrome c release from mitochondria proceeds by a two-step process. *Proc. Natl. Acad. Sci. USA* **99**, 1259–1263 (2002).
7. Nakagawa, Y. Initiation of apoptotic signal by the peroxidation of cardiolipin of mitochondria. *Ann. NY Acad. Sci.* **1011**, 177–184 (2004).
8. Kagan, V.E. *Lipid Peroxidation in Biomembranes* (CRC Press, Boca Raton, Florida, 1988).
9. Rouach, H., Clement, M., Ofranelli, M-T., Janvier, B. & Nordmann, R. Fatty acid composition of rat liver mitochondrial phospholipids during ethanol inhalation. *Biochim. Biophys. Acta* **795**, 125–129 (1984).
10. Giudetti, A.M., Siculella, L. & Gnoni, G.V. Citrate carrier activity and cardiolipin level in eel (*Anguilla anguilla*) liver mitochondria. *Comp. Biochem. Physiol. B Biochem. Mol. Biol.* **133**, 227–234 (2002).
11. Igarashi, Y. & Kimura, T. Adrenic acid in rat adrenal mitochondrial phosphatidylethanolamine and its relation to ACTH-mediated stimulation of cholesterol side chain cleavage reaction. *J. Biol. Chem.* **261**, 14118–14124 (1986).
12. Schlame, M., Beyer, K., Hayer-Hartl, M. & Klingenberg, M. Molecular species of cardiolipin in relation to other mitochondrial phospholipids. Is there an acyl specificity of interaction between cardiolipin and the ADP/ATP carrier? *Eur. J. Biochem.* **199**, 459–466 (1991).
13. Jiang, J. *et al.* Cytochrome c release is required for phosphatidylserine peroxidation during Fas-triggered apoptosis in lung epithelial A549 cells. *Lipids* **39**, 1133–1142 (2004).
14. Li, K. *et al.* Cytochrome c deficiency causes embryonic lethality and attenuates stress-induced apoptosis. *Cell* **101**, 389–399 (2000).
15. Birch-Machin, M.A. & Turnbull, D. Assaying mitochondrial respiratory complex activity in mitochondria isolated from human cells and tissues. *Methods Cell Biol.* **65**, 97–117 (2001).
16. Petit, J.M., Maftah, A., Ratinaud, M.H. & Julien, R. 10N-nonyl acridine orange interacts with cardiolipin and allows the quantification of this phospholipid in isolated mitochondria. *Eur. J. Biochem.* **209**, 267–273 (1992).
17. Dunford, H.B. *Heme Peroxidases* (John Wiley, New York, Chichester, 1999).
18. Marnett, L.J. Cyclooxygenase mechanisms. *Curr. Opin. Chem. Biol.* **4**, 545–552 (2000).
19. Tsai, A.L. *et al.* Heme coordination of prostaglandin H synthase. *J. Biol. Chem.* **268**, 8554–8563 (1993).
20. Ivancich, A., Jakopitsch, C., Auer, M., Un, S. & Obinger, C. Protein-based radicals in the catalase-peroxidase of synechocystis PCC6803: a multifrequency EPR investigation of wild-type and variants on the environment of the heme active site. *J. Am. Chem. Soc.* **125**, 14093–14102 (2003).
21. Svistunenko, D.A. Reaction of haem containing proteins and enzymes with hydroperoxides: the radical view. *Biochim. Biophys. Acta* **1707**, 127–155 (2005).
22. Svistunenko, D.A. & Cooper, C.E. A new method of identifying the site of tyrosyl radicals in proteins. *Biophys. J.* **87**, 582–595 (2004).
23. Stellwagen, E. Carboxymethylation of horse heart ferricytochrome c and cyanferricytochrome c. *Biochemistry* **7**, 2496–2501 (1968).
24. Bernad, S. *et al.* Interaction of horse heart and thermus thermophilus type c cytochromes with phospholipid vesicles and hydrophobic surfaces. *Biophys. J.* **86**, 3863–3872 (2004).
25. Tuominen, E.K., Wallace, C.J. & Kinnunen, P.K. Phospholipid-cytochrome c interaction: evidence for the extended lipid anchorage. *J. Biol. Chem.* **277**, 8822–8826 (2002).
26. Nantes, I., Zucchi, M., Nascimento, O. & Faljoni-Alario, A. Effect of heme iron valence state on the conformation of cytochrome c and its association with membrane interfaces. A CD and EPR investigation. *J. Biol. Chem.* **276**, 153–158 (2001).
27. Zucchi, M.R., Naschimento, O.R., Faljoni-Alario, A., Prieto, T. & Nantes, I.L. Modulation of cytochrome c spin stated by lipid acyl chains: a continuous-wave electron paramagnetic resonance (CW-EPR) study of haem iron. *Biochem. J.* **370**, 671–678 (2003).
28. Feix, J.B. & Kalyanaraman, B. Spin trapping of lipid-derived radicals in liposomes. *Biochim. Biophys. Acta* **992**, 230–235 (1989).
29. Malkowski, M.G., Ginell, S.L., Smith, W.L. & Garavito, R.M. The productive conformation of arachidonic acid bound to prostaglandin synthase. *Science* **289**, 1933–1937 (2000).

30. Shidoji, Y., Hayashi, K., Komura, S., Ohishi, N. & Yagi, K. Loss of molecular interaction between cytochrome c and cardiolipin due to lipid peroxidation. *Biochem. Biophys. Res. Commun.* **264**, 343–347 (1999).
31. Svistunenko, D.A. An EPR study of the peroxyl radicals induced by hydrogen peroxide in the haem proteins. *Biochim. Biophys. Acta* **1546**, 365–378 (2001).
32. Cortese, J., Voglino, A.L. & Hackenbrock, C.R. Persistence of cytochrome c binding to membranes at physiological mitochondrial intermembrane space ionic strength. *Biochim. Biophys. Acta* **1228**, 216–228 (1995).
33. Scorrano, L. *et al.* A distinct pathway remodels mitochondrial cristae and mobilizes cytochrome c during apoptosis. *Dev. Cell* **2**, 55–67 (2002).
34. Petrosillo, G., Ruggiero, F.M., Pistolese, M. & Paradies, G. Ca2+-induced reactive oxygen species production promotes cytochrome c release from rat liver mitochondria via mitochondrial permeability transition (MPT)-dependent and MPT-independent mechanisms: role of cardiolipin. *J. Biol. Chem.* **279**, 53103–53108 (2004).
35. Crouser, E.D. *et al.* Quantitation of cytochrome c release from rat liver mitochondria. *Anal. Biochem.* **317**, 67–75 (2003).
36. Ritov, V., Menshikova, E. & Kelley, D. High-performance liquid chromatography-based methods of enzymatic analysis: electron transport chain activity in mitochondria from human skeletal muscle. *Anal. Biochem.* **333**, 27–38 (2004).
37. Robinson, N.C., Zborowski, J. & Talbert, L.H. Cardiolipin-depleted bovine heart cytochrome c oxidase: binding stoichiometry and affinity for cardiolipin derivatives. *Biochemistry* **29**, 8962–8969 (1990).
38. Daum, G. Lipids of mitochondria. *Biochim. Biophys. Acta* **822**, 1–42 (1985).
39. Garcia Fernandez, M. *et al.* Early changes in intramitochondrial cardiolipin distribution during apoptosis. *Cell Growth Differ.* **13**, 449–455 (2002).
40. Cossarizza, A. *et al.* Mitochondrial functionality and mitochondrial DNA content in lymphocytes of vertically infected human immunodeficiency virus-positive children with highly active antiretroviral therapy-related lipodystrophy. *J. Infect. Dis.* **185**, 299–305 (2002).
41. Pfeiffer, K. *et al.* Cardiolipin stabilizes respiratory chain supercomlexes. *J. Biol. Chem.* **278**, 52873–52880 (2003).
42. Liu, J., Weiss, A., Durrant, D., Chi, N.W. & Lee, R.M. The cardiolipin-binding domain of Bid affects mitochondrial respiration and enhances cytochrome c release. *Apoptosis* **9**, 533–541 (2004).
43. Walensky, L. *et al.* Activation of apoptosis in vivo by a hydrocarbon-stapled BH3 helix. *Science* **305**, 1466–1470 (2004).
44. Cristea, I.M. & Degli Esposti, M. Membrane lipids and cell death: an overview. *Chem. Phys. Lipids* **129**, 133–160 (2004).
45. Epand, R.F., Martinou, J.C., Fornallaz-Mulhauser, M., Hughes, D.W. & Epand, R.M. The apoptotic protein tBid promotes leakage by altering membrane curvature. *J. Biol. Chem.* **277**, 32632–32639 (2002).
46. Gonzalvez, F. *et al.* tBid interaction with cardiolipin primarily orchestrates mitochondrial dysfunctions and subsequently activates Bax and Bak. *Cell Death Differ.* **12**, 614–626 (2005).
47. Shidoji, Y., Komura, S., Ohishi, N. & Yagi, K. Interaction between cytochrome c and oxidized mitochondrial lipids. *Subcell. Biochem.* **36**, 19–37 (2002).
48. Baines, C.P. *et al.* Loss of cyclophilin D reveals a critical role for mitochondrial permeability transition in cell death. *Nature* **434**, 658–662.
49. Nakagawa, T. *et al.* Cyclophilin D-dependent mitochondrial permeability transition regulates some necrotic but not apoptotic cell death. *Nature* **434**, 652–657 (2005).
50. Raha, S. & Robinson, B.H. Mitochondria, oxygen free radicals, and apoptosis. *Am. J. Med. Genet.* **106**, 62–70 (2001).
51. Siemankowski, L.M., Morreale, J. & Briehl, M.M. Antioxidant defenses in the TNF-treated MCF-7 cells: selective increase in MnSOD. *Free Radic. Biol. Med.* **26**, 919–924 (1999).
52. Matsura, T. *et al.* Endogenously generated hydrogen peroxide is required for execution of melphalan-induced apoptosis as well as oxidation and externalization of phosphatidylserine. *Chem. Res. Toxicol.* **17**, 685–696 (2004).
53. Chen, Y.R. *et al.* Formation of protein tyrosine ortho-semiquinone radical and nitrotyrosine from cytochrome c-derived tyrosyl radical. *J. Biol. Chem.* **279**, 18054–18062 (2004).
54. Barr, D.P., Gunther, M.R., Deterding, L.J., Tomer, K.B. & Mason, R.P. ESR spin-trapping of a protein-derived tyrosyl radical from the reaction of cytochrome c with hydrogen peroxide. *J. Biol. Chem.* **271**, 15498–15503 (1996).
55. Tyurina, Y.Y. *et al.* The plasma membrane is the site of selective phosphatidylserine oxidation during apoptosis: role of cytochrome C. *Antioxid. Redox Signal.* **6**, 209–225 (2004).
56. Nilsson, O.S. & Dallner, G. Transverse asymmetry of phospholipids in subcellular membranes of rat liver. *Biochim. Biophys. Acta* **464**, 453–458 (1977).